Journal of Human Evolution 193 (2024) 103556

Contents lists available at ScienceDirect

Journal of Human Evolution

journal homepage: www.elsevier.com/locate/jhevol

Short Communications

New hominin dental remains from Olduvai Gorge (Tanzania)

Alessandro Riga [a, *], Thomas W. Davies [b], Beatrice Azzarà [c], Giovanni Boschian [d], Costantino Buzi [e, f], Jackson S. Kimambo [g], Giorgio Manzi [h], Fidelis T. Masao [i], Amon Mgimwa [j], Happiness Nyambo [j], Paul Tafforeau [k], Wilson Jilala [l], Jacopo Moggi-Cecchi [a, *], Marco Cherin [c]

[a] Department of Biology, University of Florence, Italy
[b] Department of Human Origins, Max Planck Institute for Evolutionary Anthropology, Leipzig, Germany
[c] Department of Physics and Geology, University of Perugia, Italy
[d] Department of Biology, University of Pisa, Italy
[e] Institut Català de Paleoecologia Humana i Evolució Social (IPHES-CERCA), Tarragona, Spain
[f] Department of History and History of Art, Universitat Rovira i Virgili, Tarragona, Spain
[g] Eastern Africa Research Centre for Palaeosciences (EARCEP), Karatu, Tanzania
[h] Department of Environmental Biology, Sapienza University of Rome, Italy
[i] Department of Archaeology & Heritage, University of Dar Es Salaam, Tanzania
[j] Antiquities Division, Ministry of Natural Resources and Tourism, Tanzania
[k] European Synchrotron Radiation Facility (ESRF), Grenoble, France
[l] National Museum and House of Culture, Dar es Salaam, Tanzania

ARTICLE INFO

Article history:
Received 31 January 2024
Accepted 2 June 2024

Keywords:
Paranthropus
Homo
Early hominins
Pleistocene
Synchrotron microtomography
Teeth

1. Introduction

Olduvai Gorge (misspelling of the Maa word Oldupai), in northern Tanzania, is among the most iconic sites for the study of human evolution (Fig. 1A–C). Olduvai deposits have yielded an outstanding hominin record, spanning the last 2 Ma and including fossils attributed to at least four species: *Paranthropus boisei*, *Homo habilis*, *Homo ergaster/erectus*, and *Homo sapiens* (e.g., Leakey, 1965, 1971; Tobias, 1967, 1991; Leakey and Roe, 1995). More than 100 years of research at the site have provided valuable insights into the early evolution of hominids and the development of early human technology (Pante et al., 2020; Domínguez-Rodrigo and Baquedano, 2023; Domínguez-Rodrigo et al., 2023).

In the recent years, collaborators of the Tanzania Human Origins Research (THOR) project have recovered two hominin teeth (Fig. 2A and B) during surveys at Olduvai Gorge. In this contribution, we present the context of the findings, describe the morphology of the teeth, and analyze them to assess their identity and taxonomic affiliation. Teeth are also analyzed using synchrotron microtomography (μCT)-based methods for the first time as far as the Olduvai hominin record is concerned. Here, we provide a description and a morphometric analysis of the new dental remains, suggesting a taxonomic attribution.

1.1. Discovery and stratigraphic position

Specimen OH 92 was discovered in 2019 during surface surveys aimed at studying the Ndutu Beds in the Bell's Korongo (BK) area. The tooth laid in a small erosional channel at the base of a hill east of the BK main outcrop (2°59′45.8″S 35°19′31.8″E; Fig. 1C and E). This latter site holds significant historical importance in Olduvai as it was the first one in the Gorge to be chosen for extensive excavations by the Leakeys during the 1950s. This decision was driven by the abundant presence of megafaunal remains and their association with stone tools (Leakey, 1971). Additionally, the first partial skeleton of *P. boisei* (OH 80) was discovered in level 4 of the BK main outcrop, just above the carbonate level and Tuff IID, dated ~1.34 Ma (Upper Bed II; Dominguez-Rodrigo et al., 2013; Uribellarrea del Val and Domínguez-Rodrigo, 2017). The stratigraphic succession of the hill on which OH 92 was found includes, from bottom to top, Upper Bed II (with a clearly visible carbonate level in its uppermost part),

* Corresponding authors.
E-mail addresses: alessandro.riga@unifi.it (A. Riga), iacopo.moggicecchi@unifi.it (J. Moggi-Cecchi).

https://doi.org/10.1016/j.jhevol.2024.103556

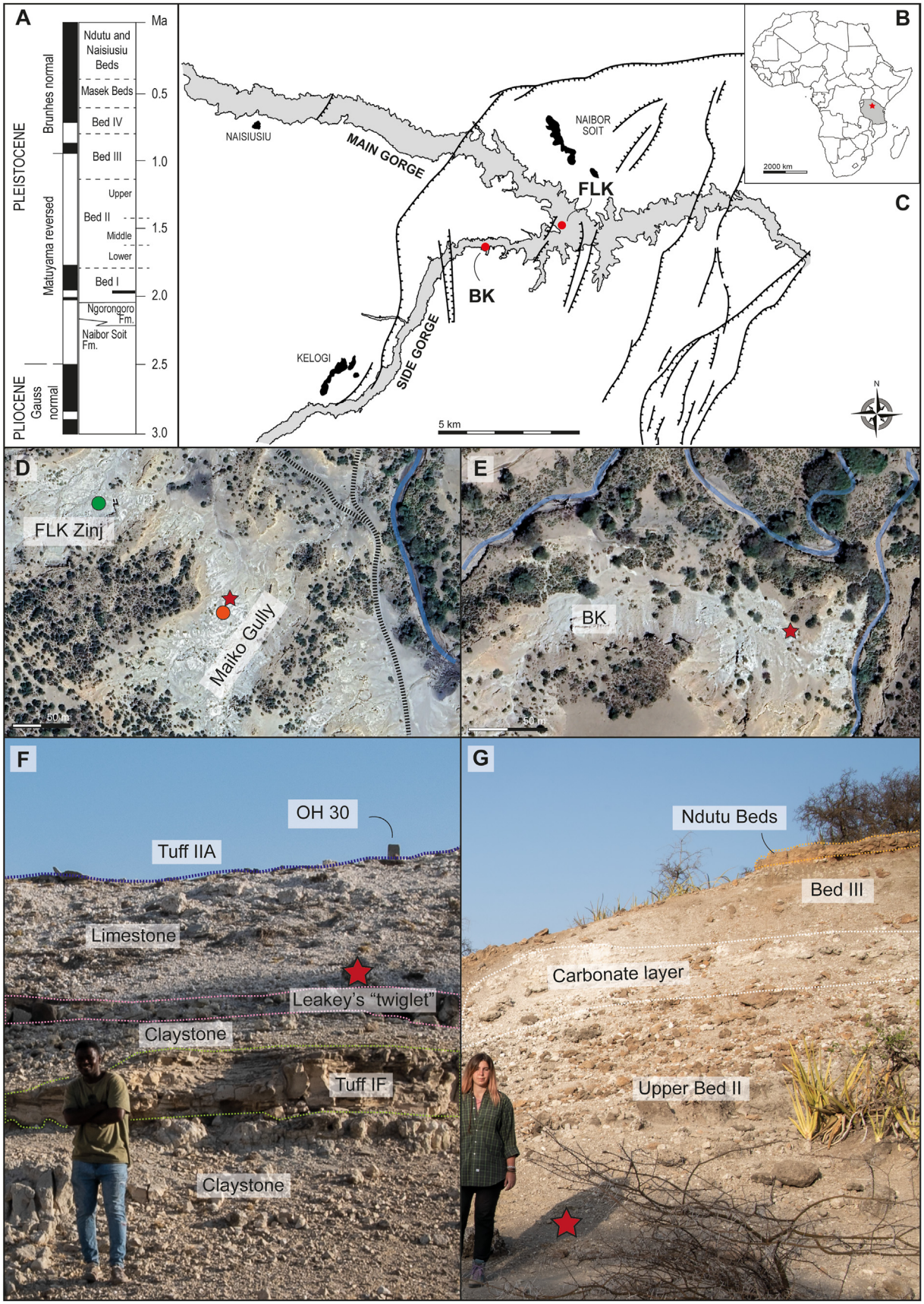

Figure 1. A) Stratigraphy of Olduvai Gorge (modified from Hay, 1976; Stanistreet et al., 2020); B) Location of Olduvai Gorge in northern Tanzania; C) Positions of the two sites (FLK and BK) within the Gorge where the teeth have been recovered; D) Location of OH 30B discovery point in the FLK Maiko Gully site, in comparison to where the OH 5 cranium ("Zinj", green dot) and OH 30 (orange dot) were discovered; E) Location of OH 92 discovery point in the BK site; F) Stratigraphy at the FLK Maiko Gully site; G) Stratigraphy at the BK site.

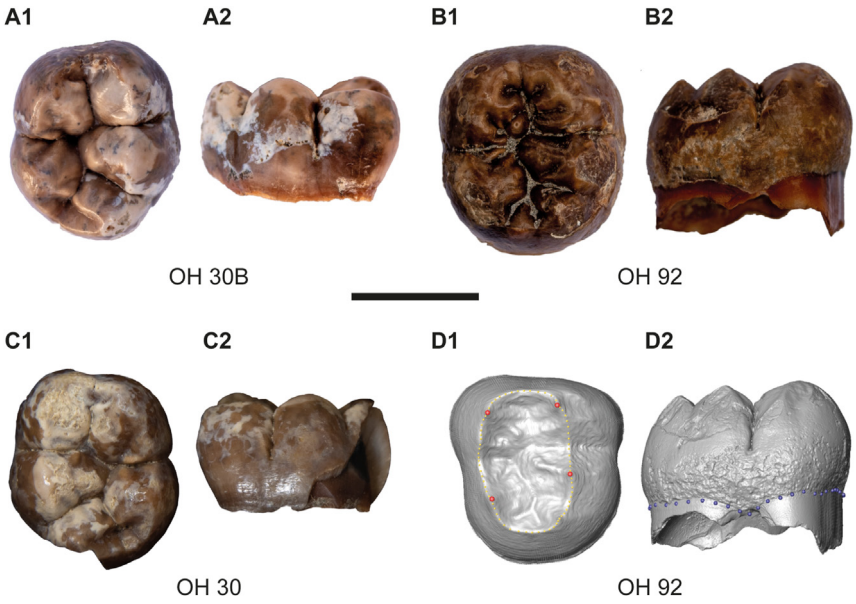

Figure 2. A) OH 30B in occlusal (A1) and buccal (A2) views; B) OH 92 in occlusal (B1) and buccal (B2) views; C) OH 30 lower left M_1 in occlusal (C1) and buccal (C2) views; D) Set of landmarks (red dots) and semilandmarks (yellow dots) on the enamel–dentine junction (EDJ) (D1) and set of semilandmarks (blue dots) placed on the cervical line (D2) of OH 92. Scale bar: 10 mm. (For interpretation of the references to color in this figure legend, the reader is referred to the web version of this article.)

Bed III, and the Ndutu Beds (Fig. 1G). Therefore, OH 92 could come from any of these beds. However, the brown color of the specimen associated with the strong mineralization points toward a possible origin from Upper Bed II (dental remains from Bed III are normally much darker or even black in color).

Specimen OH 30B was discovered in 2021 in the Maiko Gully at the Frida Leakey Korongo (FLK) site, specifically in geological locality 45c (Hay, 1976). The location of the find (2°59′25.5″S 35°20′59.0″E; Fig. 1C and D) is very close to where OH 30 was recovered in 1969 (Leakey, 1971). As we will demonstrate, there is compelling evidence that the new tooth belongs to the same individual, hence the code OH 30B. The stratigraphic position of OH 30B (Fig. 1F) aligns with the interpretation provided by Leakey (1971), suggesting an age spanning from 1.8 Ma (dating of Tuff IF; Deino et al., 2021) to either 1.756 Ma or 1.677 Ma (dating of Tuff IIA; McHenry and Stanistreet, 2018). Within the same deposits in the Maiko Gully, the Leakeys recovered OH 17—an isolated deciduous molar—and OH 16, which comprises multiple cranial fragments, and upper and lower teeth initially referred to *H. erectus* (Leakey and Leakey, 1964), later to *H. habilis* (Leakey et al., 1964) or even cf. *Australopithecus* (Leakey, 1971). Contemporary consensus now typically attributes OH 16 to *H. habilis*, although recent μCT-based analysis recognizes an intermediate morphology between early *Homo* and more derived species in OH 16, suggesting a revision of the *H. habilis* hypodigm (Davies et al., 2024).

2. Materials and methods

2.1. Comparative material

The original material of OH 30 was analyzed at the National Museum of Tanzania in Dar es Salaam, where also OH 30B and OH 92 are curated.

Linear measurements and cusp areas were compared with literature data on African Pleistocene specimens belonging to the genera *Homo*, *Paranthropus*, and *Australopithecus* (Wood, 1991; Grine et al., 2019). The complete list of the specimens and their measurements are listed in Supplementary Online Material (SOM Table S1). Average enamel thickness (AET) and relative enamel thickness (RET) have been compared with a subsample of the data published by Skinner et al. (2015) (SOM Table S2).

The comparative sample for geometric morphometrics (GM) includes three-dimensional (3D) models of hominin molars from Africa belonging to the genera *Homo*, *Paranthropus*, and *Australopithecus* (SOM Table S3).

2.2. Acquisition of digital images and 3D models

Digital images of the two specimens presented in this paper were acquired through synchrotron light at the European Synchrotron Radiation Facility in Grenoble. All the relevant parameters for the scanning and reconstruction are given in SOM Table S4. Microtomographic scans of the comparative sample were obtained using either a SkyScan 1172 or SkyScan 1173 at 100–130 kV and 90–130 microA, a BIR ACTIS 225/300 scanner at 130 kV and 100–120 microA, or a Diondo d3 at 100–140 kv and 100–140 microA and reconstructed as 16-bit Tag Image File Format (TIFF) stacks with an isometric voxel resolution ranging from 13 to 45 μm. The reconstructed TIFF stacks were filtered using only a mean-of-least-variance filter (with a kernel size one), or a 3D median filter followed by a mean-of-least-variance filter (both with a kernel size of three), implemented using the MIA open-source software (Wollny et al., 2013). Filtered image stacks were used to segment the different dental tissues (pulp, dentine and enamel). Segmentation was performed using a seed-growing watershed algorithm used via a custom plugin for Avizo 6.3 (Visualization Sciences Group), before being checked manually. After segmentation, a triangle-based surface model of the enamel–dentine junction (EDJ)

The positions of the teeth are indicated by stars. Abbreviations: BK = Bell's Korongo; FLK = Frida Leakey Korongo. (For interpretation of the references to color in this figure legend, the reader is referred to the web version of this article.)

surface was produced and saved in polygon file format (.ply). In some cases within the comparative sample, dental wear had removed the dentine horn tips; where this wear was minimal, the missing portion of the dentine horn was reconstructed following previously published procedures (Skinner, 2008; Davies et al., 2024). This was restricted to cases in which the wear was less than wear level 3 as defined by Molnar (1971), and when the observer was confident of the reconstruction using experience, anatomical knowledge, and the preserved EDJ morphology. The reconstruction procedure was completed using surface modification tools in Geomagic Studio 2014 (https://www.geomagic.com), beginning with the 'fill holes' function, before manual adjustments using the 'sculpt knife' function to infer the shape of the tip from the preserved anatomy of the dentine horn. Where necessary, the positions of landmarks on the cusp tops were also adjusted manually in Avizo 6.3. Neither specimen presented in this paper required reconstruction, but examples of these in comparative sample specimens are available in Davies et al. (2024).

The 3D models of OH 30B and OH 92 have been uploaded to MorphoSource and are available at https://n2t.net/ark:/87602/m4/635203 and https://n2t.net/ark:/87602/m4/635210, respectively.

2.3. Linear measurements and cusp areas, and two-dimensional enamel thickness

Mesio-distal (MD) and bucco-lingual (BL) crown diameters of both teeth were measured using a digital caliper following Wood (1991). Cusp and crown areas were measured on occlusal pictures using the software ImageJ (https://imagej.nih.gov/ij) and following standard protocols (Wood and Abbott, 1983). Relative cusp area was calculated as percentage of total crown area. The results of these analyses are presented in SOM Figs. S1–S5. Furthermore, we calculated AET and RET following Skinner et al. (2015; SOM Fig. S6).

2.4. Geometric morphometrics

We used a GM dataset on the EDJ (Fig. 2D), following the protocol for molars outlined in Davies et al. (2024), defined by four type-2 landmarks on the horn tips of the four principal cusps (metaconid, protoconid, hypoconid, and entoconid), four sets of 20 semilandmarks between each principal cusp, along the marginal ridges of the EDJ, and a set of 40 semilandmarks along the cervix. Landmarks along the marginal ridges were placed beginning at the protoconid and continuing mesially, eventually returning to the protoconid, whereas cervix landmarks were placed on the mesiobuccal corner of the crown, below the protoconid, and continuing mesially. EDJ marginal ridge landmarks were placed directly on the EDJ model, whereas cervix landmarks were placed on an isosurface rendering of the unfiltered TIFF stack or, where this was not possible, directly on the image stack. Missing portions of the cervix contour have been estimated where the original position of the cervix was clear. Semilandmarks were allowed to slide along their curves, minimizing the bending energy of the thin-plate spline interpolation function calculated between each specimen and the Procrustes average for the sample (Gunz et al., 2005; Gunz and Mitteroecker, 2013). Sliding was performed twice, with landmarks projected back on to the curves after each step, after which landmarks were considered geometrically homologous. We then performed generalized Procrustes analysis translating, rotating, and scaling the landmark configurations, analyzing the data in the shape space and extracting the values of the centroid size. Afterward, we performed a principal component analysis (PCA) on the Procrustes coordinates of each specimen in shape space. Shape differences between groups were visualized using wireframe models of shape changes across the first three principal components (PCs).

We conducted the analyses using the complete comparison sample and a subsample composed only of those species whose presence is recognized in Olduvai. Here, we present the results of the former analysis, whereas the latter is presented in SOM Fig. S7.

3. Results

3.1. Anatomical description

OH 30B This tooth is the intact crown of a lower right (first?) molar (Fig. 2A). It is well preserved apart from some taphonomic damage on the distal face, where tiny flakes of enamel are also missing at the base of the crown. The tooth was unerupted. Crown formation was complete with a couple of mm of root formed. The occlusal outline is oval, with some distal projection. The five main cusps are well delineated. The metaconid is the largest cusp, followed by protoconid, hypoconid, entoconid, and hypoconulid. The cusp tips are positioned near the edge of the occlusal profile creating a large occlusal basin. The primary fissure pattern is evident, with a metaconid–hypoconid contact. The mesial marginal ridge is low and thick and bears a tiny cuspulid that flows into a large mesial fovea, occupying most of it. The central fovea is broad and shallow, with well-delineated buccal and lingual grooves. The distal fovea is also large and deep, bounded by a thick and low distal marginal ridge. No accessory cusps are evident, except for an incipient cuspulid on the postentocristid. The mesial face shows a small concavity in its midpart—possibly an hypoplastic pit. The buccal face shows a mild occlusocervical convexity, and it has a deep and long mesiobuccal groove, ending in its midpart. The deep distobuccal groove is much shorter. The lingual face has a more marked occlusocervical convexity, and it shows a very short lingual groove, ending gradually. The distal face is featureless apart from the taphonomic damage.

OH 92 This tooth is the intact crown of a lower right (second?/third?) molar (Fig. 2B). Preservation is good but taphonomic damage, of different extent, is evident on the mesial, distal, buccal, and lingual faces. The tooth was unerupted. Crown formation was complete with 5 mm of root formed, as measured on the mesial face. The forming root is largely intact. The occlusal outline is almost square, with rounded corners. The main cusps are well delineated. The metaconid is the largest cusp, followed by protoconid, entoconid, hypoconid, and hypoconulid. The cusp tips are positioned near the center of the occlusal profile creating a small occlusal basin. The primary fissure pattern is evident, with a metaconid–hypoconid contact. The mesial marginal ridge is thick and high, incised in its midportion by a deep groove that moves into the mesial fovea. This groove also delineates two small cuspulids of different sizes. The central fovea is broad and shallow. The buccal and lingual grooves are evident, as are the other, additional, grooves on the occlusal sides of the main cusps. Near the base of the metaconid, two of these grooves delineate a tiny cuspulid on the ridge that moves from the cusp tip to the central fovea. The distal fovea is large and deep, partly occupied by a distinct C6 and bounded by a thick and high distal marginal ridge. The buccal face shows a notable occlusocervical convexity, and it has a deep and long mesiobuccal groove, ending in its midpart. The distobuccal groove is obscured by taphonomic damage. The lingual face has a marked occlusocervical convexity, and it shows a very short lingual groove. The mesial and distal faces are featureless apart from the taphonomic damage.

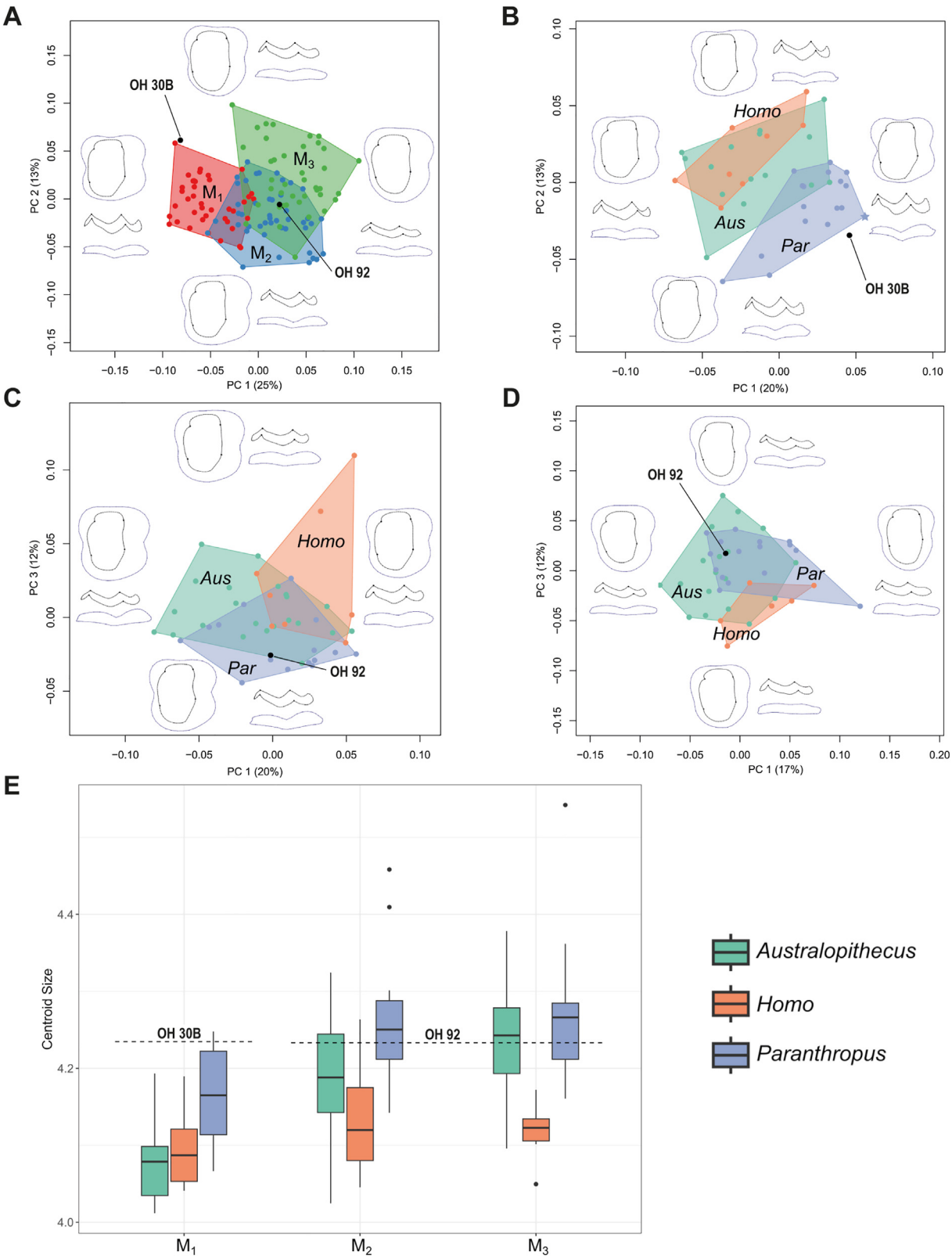

Figure 3. Results of principal component analyses (PCAs) on the extended sample shape space. A) OH 30B and OH 92 compared to other fossil M_1, M_2, and M_3; B) Position of OH 30B relative to other M_1 attributed to the genera *Homo*, *Paranthropus*, and *Australopithecus* (OH 30 is marked by a star); C) Position of OH 92 relative to other M_2 attributed to the genera *Homo*, *Paranthropus*, and *Australopithecus*; D) Position of OH 92 relative to other M_3 attributed to the genera *Homo*, *Paranthropus*, and *Australopithecus*; E) Centroid Size of OH 30B and OH 92 compared to M_1, M_2, and M_3 attributed to the genera *Homo*, *Paranthropus*, and *Australopithecus*. (For interpretation of the references to color in this figure, the reader is referred to the Web version of this article.)

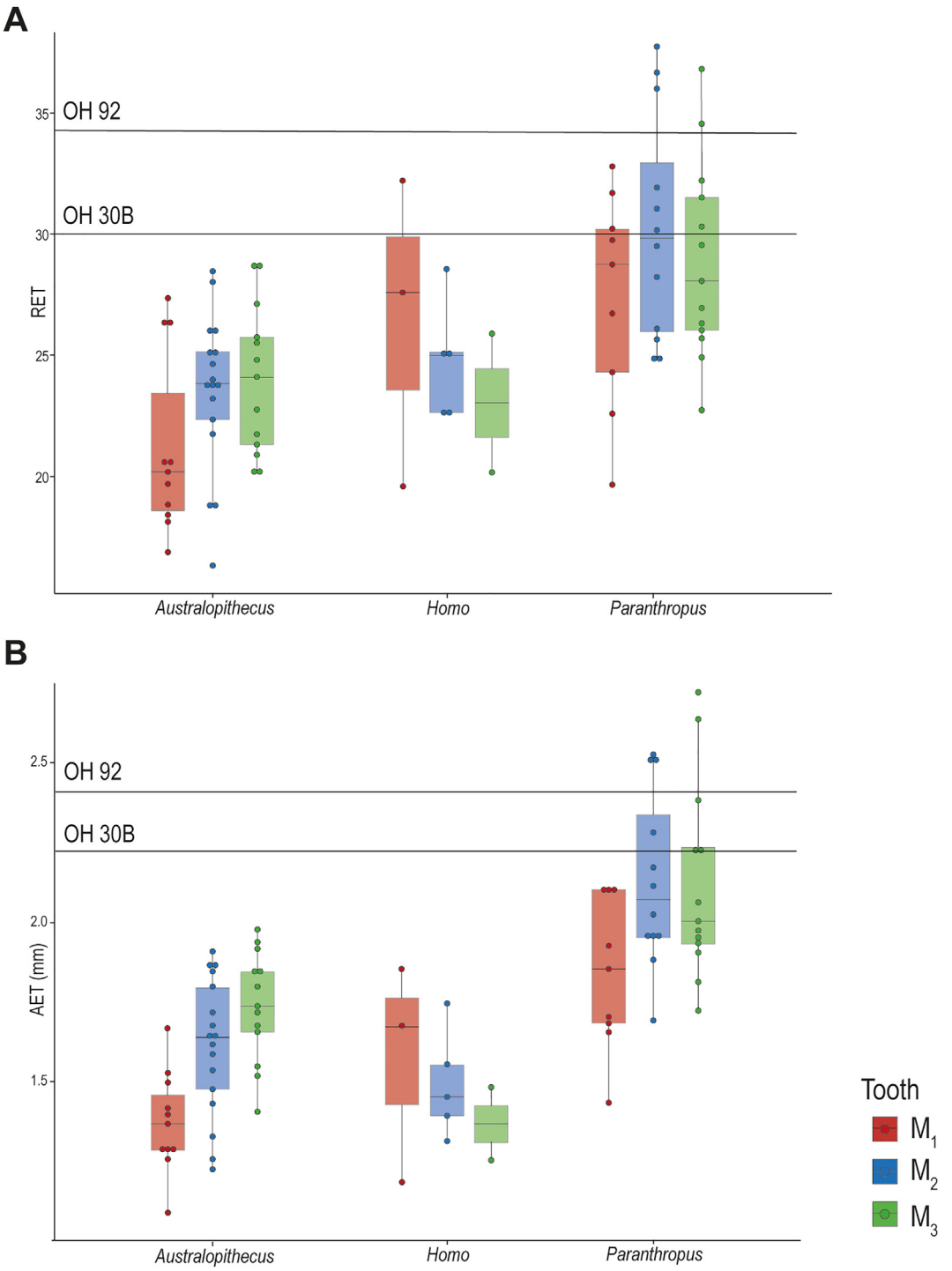

Figure 4. Results of the analysis of enamel thickness. A) Relative enamel thickness (RET) and B) Average enamel thickness (AET) in OH 30B and OH 92 compared to a sample of *Australopithecus*, *Homo*, and *Paranthropus* lower molars. (For interpretation of the references to color in this figure, the reader is referred to the Web version of this article.)

3.2. Position in the tooth row

The results of the PCA indicate that the different molars cluster in distinct areas within the shape space, although there is some degree of overlap between all three molar positions (Fig. 3A). The first three PCs account for 46% of the total variance. Variation along PC1 is mainly associated with dentine body height and expression of the cusps. PC2 describes the expansion of the dentine body on the buccal side and the relative size of the occlusal basin. PC3 is related to the shape of the cervical contour.

The position of OH 30B on the plot is proximate to M_1 but distant from M_2 and M_3, confidently suggesting that it is an M_1. Conversely, the position of OH 92 is less conclusive as it falls within the variability range of both M_2 and M_3. In subsequent analyses, we have considered OH 30B as an M_1 and OH 92 as either an M_2 or an M_3.

3.3. Taxonomy

When OH 30B is compared to other M_1s, there is a considerable overlap in the shape space between *Homo* and *Australopithecus*; however, teeth attributed to *Paranthropus* exhibit clear separation along PC1 and PC2. The first three PCs collectively account for 66% of the total variance.

Notably, OH 30B is situated at the edge of the *Paranthropus* distribution, on the opposite side of the plot to the other genera (Fig. 3B). It plots closely to the left M_1 of OH 30 (and OH 30 is the closest specimen to OH 30B in Procrustes distances), suggesting a similar EDJ shape.

In the case of OH 92, its position in the tooth row is less clear. Therefore, we compared it to a sample of M_2 (Fig. 3C) and M_3 (Fig. 3D). For the M_2 sample, the first three PCs explain 46% of the total variance, whereas for the M_3 sample, they account for 43% of the total variance. In both cases, PC3 proves instrumental in distinguishing among the genera, with OH 92 falling within the variability of *Paranthropus* and *Australopithecus*, distinctly outside the variability observed in *Homo*.

The analysis of centroid size corroborates the aforementioned observations (Fig. 3E): the size of OH 30B aligns with that of other *Paranthropus* teeth, lying outside the variability observed in both *Homo* and *Australopithecus* M_1s. Conversely, the size of OH 92 is consistent with those of *Australopithecus* and *Paranthropus* but notably larger than that of *Homo*, whether compared to M_2 or M_3. The analysis of enamel thickness gives different patterns for RET (Fig. 4A) and AET (Fig. 4B). OH 92 RET is in the range of *Paranthropus*, which is well above the values of *Homo* and *Australopithecus*. OH 30B RET falls in the range of *Paranthropus* and in the higher part of the range of *Homo*. AET (Fig. 4B) points toward an attribution of both teeth to *Paranthropus*.

As for the analyses presented in the SOM Figs. S2–S5, linear measurements (SOM Fig. S2A–C) suggest that OH 30B is a *Paranthropus*, whereas the position of OH 92 is less conclusive. Cusp areas (SOM Fig. S3) of OH 30B suggest an attribution to *Paranthropus*. All the cusp areas fall within the range observed in *Paranthropus*, whereas some variably fall outside the range observed in other groups. The analysis of cusp areas in OH 92 (SOM Figs. S4–S5) is less conclusive but still compatible with an attribution to the genus *Paranthropus*.

4. Discussion and conclusions

The observations of the morphological features and the analyses presented here, as well as in the SOM, agree that OH 30B is most likely a lower first molar, whereas OH 92 is either a lower second or third molar.

Their morphology differs significantly at both the EDJ and the outer enamel surface (OES). At the EDJ (SOM Fig. S8), OH 92 has lower dentine horns placed more centrally than OH 30B, resulting in a smaller occlusal basin. In OH 30B, the distal fovea is larger and mesially well delimited by a steep entoconid–hypoconulid crest. The absence of this feature on the EDJ of OH 92 creates a distally tapering occlusal profile. On the EDJ of OH 92, two bulges are present: one near the base of the metaconid corresponding to the cuspulid at the OES and one on the marginal ridge corresponding to the C6 at the OES. These differences are also observable at the OES. The GM analyses suggest assigning OH 30B to the genus *Paranthropus* and OH 92 to either *Paranthropus* or *Australopithecus*. Analyses of the cusp areas and enamel thickness (AET and RET) point toward an attribution of OH 92 to the former genus. Considering also that there is still no evidence of *Australopithecus* fossils in Olduvai (but see Clarke et al., 2021, who suggest that some of the specimen that we included in the Early *Homo* sample are indeed *Australopithecus africanus*), we deem both teeth to belong to the genus *Paranthropus*.

Some of the differences between OH 30B and OH 92 are likely to represent metameric differences in the tooth row. In South African *Paranthropus robustus*, compared to M_1, the M_2 exhibits a less frequent expression of the hypoconulid, a reduction in the height of dentine horns, and a more central position of the entoconid horn; compared to M_3, in the M_2, the hypoconid is more centrally placed (Pan et al., 2017). All these features are possibly present in the East African *Paranthropus*, although specific studies on metameric variation in this group are lacking, and reflect some of the differences between OH 30B (M_1) and OH 92 (M_2 or M_3), contributing to the flattened appearance of the OES and a reduced occlusal basin in OH 92.

As mentioned in the introduction, OH 30B was discovered a few meters away from the location where OH 30 was found in 1969 (Leakey, 1971). The specimen OH 30 consists of several isolated teeth of a subadult individual along with some cranial fragments (Tobias, 1991). Among these teeth is a lower left M_1 (Fig. 2C), a well-preserved tooth, except for a fragment of enamel missing in the distal portion of the crown. As OH 30B, it is unerupted, featuring a complete crown and a couple of mm of root formed. The morphology closely resembles that of OH 30B, with well-defined major cusps and the same fissure pattern. Additionally, the two teeth share very similar crown measurements (see SOM Table S1), and the quantitative analysis places them next to each other (e.g., Fig. 3B). Based on these observations, we conclude that OH 30B is the antimere of the OH 30 lower left first molar.

These findings nearly double the sample size for *Paranthropus* lower molars from Olduvai Gorge, which is currently composed by only the other three lower molars: OH 26 (left M_3; Leakey, 1971; Tobias, 1991), OH 30 (left M_1; Leakey, 1971; Tobias, 1991), and OH 38 (left M_2; Tobias, 1991).

Declaration of competing interest

There is no conflict of interest.

CRediT authorship contribution statement

Alessandro Riga: Writing – review & editing, Writing – original draft, Visualization, Supervision, Methodology, Investigation, Formal analysis, Conceptualization. **Thomas W. Davies:** Writing – review & editing, Writing – original draft, Visualization, Methodology, Investigation, Formal analysis, Conceptualization. **Beatrice Azzarà:** Writing – original draft, Visualization, Investigation. **Giovanni Boschian:** Writing – original draft, Supervision, Investigation. **Costantino Buzi:** Writing – review & editing, Software, Formal analysis, Conceptualization. **Jackson S. Kimambo:** Writing – review & editing, Investigation. **Giorgio Manzi:** Writing – review & editing, Supervision, Project administration, Funding acquisition. **Fidelis T. Masao:** Writing – review & editing. **Amon Mgimwa:** Supervision, Resources, Project administration. **Happiness Nyambo:** Supervision, Resources, Project administration. **Paul Tafforeau:** Writing – review & editing, Methodology, Formal analysis. **Wilson Jilala:** Resources, Data curation. **Jacopo Moggi-Cecchi:** Writing – review & editing, Writing – original draft, Supervision, Methodology, Investigation, Conceptualization. **Marco Cherin:** Writing – review & editing, Writing – original draft, Visualization, Supervision, Project administration, Investigation, Funding acquisition, Conceptualization.

Acknowledgments

This research was supported by the School of Paleoanthropology of the University of Perugia (responsible MC), the Italian Ministry of Foreign Affairs and International Cooperation (Italian Archaeological, Anthropological and Ethnological Missions Abroad program; grant numbers: Arc-1022, Arc-1174, Arc-2553; responsible GM), and the Italian Ministry of University and Research (PRIN 2022 funded by Next Generation EU through PNRR; grant number: 2022KJB743; responsible MC). We thank all the Italian and Tanzanian participants in the field-trips of the School of Paleoanthropology (http://www.paleoantropologia.it) and Tanzania Human Origins Research (THOR) project (http://thorproject.it). The Maasai Community and Leakey Camp staff are equally acknowledged. In particular, we thank Elias Burra and student Raymond Matei for the discoveries of OH 30B and OH 92, respectively. We acknowledge the Tanzania Commission for Science and Technology (COSTECH), the Antiquities Division of the Ministry of Natural Resources and Tourism, the Ngorongoro Conservation Area Authority (NCAA), and the National Museum of Tanzania (NMT) for research permits and all their support. For access to computed tomography (CT) scans of comparative material, we would like to thank Emma Mbua and Samuel Muteti (National Museums of Kenya), Audax Mabulla (National Museum of Tanzania), Agness Gidna (Department of Cultural Heritage, Ngorongoro Conservation Area Authority), COSTECH, Metasebia Endalemaw and Yared Assefa (Ethiopian Heritage Authority), Bernhard Zipfel and Sifelani Jira (Evolutionary Studies Institute, University of the Witwatersrand), and Miriam Tawane (Ditsong Museum). For micro-CT-scanning and technical assistance, we thank Kudakwashe Jakata, David Plotzki, and Heiko Temming.

Supplementary Online Material

Supplementary online material to this article can be found online at https://doi.org/10.1016/j.jhevol.2024.103556.

References

Clarke, R.J., Pickering, T.R., Heaton, J.L., Kuman, K.K., 2021. The Earliest South African Hominids. Annu. Rev. Anthropol. 50, 125–143.

Davies, T.W., Gunz, P., Spoor, F., Alemseged, Z., Gidna, A., Hublin, J.J., Kimbel, W.H., Kullmer, O., Plummer, W.P., Zanolli, C., Skinner, M.M., 2024. Dental morphology in *Homo habilis* and its implications for the evolution of early *Homo*. Nat. Commun. 15, 286. https://doi.org/10.1038/s41467-023-44375-9.

Deino, A.L., Heil, C., King, J., McHenry, L.J., Stanistreet, I.G., Stollhofen, H., Njau, J.K., Mwankunda, J., Schick, K.D., Toth, N., 2021. Chronostratigraphy and age modeling of Pleistocene drill cores from the Olduvai Basin, Tanzania (Olduvai Gorge Coring Project). Palaeogeogr. Palaeoclimatol. Palaeoecol. 571, 109990. https://doi.org/10.1016/j.palaeo.2020.109990.

Domínguez-Rodrigo, M., Baquedano, E., 2023. Olduvai Gorge, Tanzania. In: Beyin, A., Wright, D.K., Wilkins, J., Olszewski, D.I. (Eds.), Handbook of Pleistocene Archaeology of Africa. Springer, Cham, pp. 1133–1151. https://doi.org/10.1007/978-3-031-20290-2_74.

Dominguez-Rodrigo, M., Pickering, T.R., Baquedano, E., Mabulla, A., Mark, D.F., Musiba, C., Bunn, H.T., Uribelarrea, D., Smith, V., Diez-Martin, F., Pérez-Gonzáles, A., Sánchez, P., Santonja, M., Barboni, D., Gidna, A., Ashley, G., Yravedra, J., Heaton, J.L., Arriaza, M.C., 2013. First partial skeleton of a 1.34-million-year-old *Paranthropus boisei* from Bed II, Olduvai Gorge, Tanzania. PLoS One 8, e80347. https://doi.org/10.1371/journal.pone.0080347.

Domínguez-Rodrigo, M., Uribelarrea, D., Diez-Martín, F., Mabulla, A., Gidna, A., Cobo-Sánchez, L., Martín-Perea, D.M., Organista, E., Barba, R., Baquedano, E., 2023. Earliest Acheulian paleolandscape reveals a 1.7 million-year-old megasite at Olduvai Gorge (Tanzania). Quat. Sci. Rev. 316, 108262. https://doi.org/10.1016/j.quascirev.2023.108262.

Grine, F.E., Leakey, M.G., Gathago, P.N., Brown, F.H., Mongle, C.S., Yang, D., Jungers, W.L., Leakey, L.N., 2019. Complete permanent mandibular dentition of early *Homo* from the upper Burgi Member of the Koobi Fora Formation, Ileret, Kenya. J. Hum. Evol. 131, 152–175. https://doi.org/10.1016/j.jhevol.2019.03.017.

Gunz, P., Mitteroecker, P., Bookstein, F.L., 2005. Semilandmarks in three dimensions. In: Slice, D.E. (Ed.), Modern Morphometrics in Physical Anthropology. Springer, Boston, pp. 73–98. https://doi.org/10.1007/0-387-27614-9_3.

Gunz, P., Mitteroecker, P., 2013. Semilandmarks: A method for quantifying curves and surfaces. Hystrix It. J. Mammal. 24, 103–109. https://doi.org/10.4404/hystrix-24.1-6292.

Hay, R.L., 1976. The Geology of Olduvai Gorge. University of California Press.

Leakey, L.S.B., 1965. Olduvai Gorge: Volume 1. Cambridge University Press, Cambridge.

Leakey, L.S., Leakey, M.D., 1964. Recent discoveries of fossil hominids in Tanganyika: At Olduvai and near Lake Natron. Nature 202, 5–7. https://doi.org/10.1038/202005a0.

Leakey, L.S., Tobias, P.V., Napier, J.R., 1964. A new species of the genus *Homo* from Olduvai Gorge. Nature 202, 7–9. https://doi.org/10.1038/202005a0.

Leakey, M., 1971. Olduvai Gorge: Volume 3, Excavations in Beds I and II, 1960-1963. Cambridge University Press, Cambridge.

Leakey, M., Roe, D., 1995. Olduvai Gorge: Volume 5, Excavations in Beds III, IV and the Masek Beds. Cambridge University Press, Cambridge.

McHenry, L.J., Stanistreet, I.G., 2018. Tephrochronology of bed II, Olduvai gorge, Tanzania, and placement of the Oldowan–Acheulean transition. J. Hum. Evol. 120, 7–18. https://doi.org/10.1016/j.jhevol.2017.12.006.

Molnar, S., 1971. Human tooth wear, tooth function and cultural variability. Am. J. Phys. Anthropol. 34, 175–189. https://doi.org/10.1002/ajpa.1330340204.

Pan, L., Thackeray, J.F., Dumoncel, J., Zanolli, C., Ottlé, A., de Beer, Frikkie, Hoffman, J., Duployer, B., Tenailleau, C., Braga, J., 2017. Intra-individual metameric variation expressed at the enamel-dentine junction of lower post-canine dentition of South African fossil hominins and modern humans. Am. J. Phys. Anthropol. 163, 806–815. https://doi.org/10.1002/ajpa.23240.

Pante, M., de La Torre, I., d'Errico, F., Njau, J., Blumenschine, R., 2020. Bone tools from Beds II–IV, Olduvai Gorge, Tanzania, and implications for the origins and evolution of bone technology. J. Hum. Evol. 148, 102885. https://doi.org/10.1016/j.jhevol.2020.102885.

Skinner, M., 2008. Enamel-Dentine Junction Morphology in Extant Hominoid and Fossil Hominin Lower Molars. The George Washington University.

Skinner, M.M., Alemseged, Z., Gaunitz, C., Hublin, J.J., 2015. Enamel thickness trends in Plio-Pleistocene hominin mandibular molars. J. Hum. Evol. 85, 35–45. https://doi.org/10.1016/j.jhevol.2015.03.012.

Stanistreet, I.G., Stollhofen, H., Deino, A.L., McHenry, L.J., Toth, N.P., Schick, K.A., Njau, J.K., 2020. New Olduvai Basin stratigraphy and stratigraphic concepts revealed by OGCP cores into the Palaeolake Olduvai depocentre, Tanzania. Palaeogeogr. Palaeoclimatol. Palaeoecol. 554, 109751. https://doi.org/10.1016/j.palaeo.2020.109751.

Tobias, P.V., 1967. Olduvai Gorge: Volume 2. Cambridge University Press, Cambridge.

Tobias, P.V., 1991. The skulls, endocasts, and teeth of *Homo habilis*. In: Olduvai Gorge, Volume IV. Cambridge University Press, Cambridge.

Uribellarrea del Val, D., Domínguez-Rodrigo, M., 2017. Geoarchaeology in a meandering river: A study of the BK site (1.35 Ma), Upper Bed II, Olduvai Gorge (Tanzania). Palaeogeogr. Palaeoclimatol. Palaeoecol. 488, 76–83. https://doi.org/10.1016/j.palaeo.2017.05.006.

Wollny, G., Kellman, P., Ledesma-Carabayo, M.J., Skinner, M.M., Hublin, J.J., Hierl, T., 2013. MIA-A free and open source software for gray scale medical image analysis. Source Code Biol. Med. 8, 20. https://doi.org/10.1186/1751-0473-8-20.

Wood, B.A., 1991. Koobi Fora Research Project Vol. 4. Hominid Cranial Remains. Oxford University Press.

Wood, B.A., Abbott, S.S., 1983. Analysis of the dental morphology of Plio-Pleistocene hominids. I. Mandibular molars: Crown area measurements and morphological traits. J. Anat. 136, 197–219.